Applied Surface Science 574 (2022) 151587

Contents lists available at ScienceDirect

Applied Surface Science

journal homepage: www.elsevier.com/locate/apsusc

Full Length Article

The role of electrolysis and enzymatic hydrolysis treatment in the enhancement of the electrochemical properties of 3D-printed carbon black/poly(lactic acid) structures

Adrian Koterwa [a,1], Iwona Kaczmarzyk [b,1], Szymon Mania [c], Mateusz Cieslik [c,d], Robert Tylingo [c], Tadeusz Ossowski [a], Robert Bogdanowicz [b], Paweł Niedziałkowski [a], Jacek Ryl [d,*]

[a] Department of Analytical Chemistry, University of Gdansk, Wita Stwosza 63, 80-308 Gdansk, Poland
[b] Department of Metrology and Optoelectronics and Advanced Materials Center, Gdansk University of Technology, Narutowicza 11/12, 80-233 Gdansk, Poland
[c] Faculty of Chemistry, Gdansk University of Technology, Narutowicza 11/12, 80-233 Gdansk, Poland
[d] Institute of Nanotechnology and Materials Engineering and Advanced Materials Center, Gdansk University of Technology, Narutowicza 11/12, 80-233 Gdansk, Poland

ARTICLE INFO

Keywords:
Polymer-matrix composite
Electrochemical behavior
Surface treatment
3D printing
Enzymatic hydrolysis

ABSTRACT

Additive manufacturing, also known as 3D printing, is beginning to play an unprecedented role in developing many applications for industrial or personalized products. The conductive composite structures require additional treatment to achieve an electroactive surface useful for electrochemical devices. In this paper, the surfaces of carbon black/poly(lactic acid) CB-PLA printouts were activated by electrolysis or enzymatic digestion with proteinase K, or a simultaneous combination of both. The proposed modification protocols allow the tailoring of electrochemically active surfaces and electron transfer kinetics determined by electrochemical techniques (CV, EIS) by $[Fe(CN)_6]^{4-/3-}$ redox probe. X-ray photon spectroscopy and SEM imaging were applied to determine the delivered surface chemistry. CB-PLA hydrolysis under alkaline conditions and anodic polarization greatly impacted the charge transfer kinetics. The enzymatic hydrolysis of PLA with proteinase K led to highly efficient results, yet requires an unsatisfactory prolonged activation duration of 72 h, which can be efficiently reduced by electrolysis carried out in the presence of the enzyme. Our studies hint that the activation protocol originates from surface electropolymerization rather than a synergistic interaction between the electrolysis and enzymatic hydrolysis. The detailed mechanism of CB-PLA hydrolysis supported by electrolysis is a promising new route to achieve time-efficient and environmentally-friendly activation procedure.

1. Introduction

The advent of Additive Manufacturing (AM), also known as 3D printing, has an unprecedented impact on development in various fields, including science, engineering and industry. As a result, affordable desktop three-dimensional printers, based on fused deposition modeling (FDM), have become a popular tool for fabricating personalized consumer products. Fused deposition modeling or fused filament fabrication (FFF) are the most commonly utilized and commercially successful methods due to their low cost, easy-to-use interface and graphic software. Furthermore, the expiration of the original FDM patents has led to a growing market in extrusion-based printers. The development of desktop extrusion-based printers opens up ways to approach new areas, including biomedical sensors [1], electronics, chemistry [2], pharmaceutics [3] and medicine [4], partly because they are inexpensive to own and operate. Furthermore, they are eco-friendly, encourage fast prototyping, and give the possibility to design objects featuring specific shapes.

Polylactic acid (PLA) is one of the most promising materials used nowadays. It is biodegradable, recyclable, highly processable, and degrades into non-toxic products [5,6]. High conductive fillers such as graphene, carbon black (CB) and carbon nanotubes (CNT), dispersed in the thermoplastic polymer matrix, are used to achieve electrically conductive filaments. Developments in FFF and commonly available conductive filaments allow the fabrication of sensors for various applications, flow cells [7], and microfluidic devices [8]. 3D printed

* Corresponding author.
E-mail address: jacek.ryl@pg.edu.pl (J. Ryl).
[1] These authors contributed equally to the manuscript.

https://doi.org/10.1016/j.apsusc.2021.151587
Received 15 June 2021; Received in revised form 24 September 2021; Accepted 9 October 2021
Available online 24 October 2021

electrodes have been used for numerous electrochemical applications, including sensing dopamine, catechol, 2,5,6-trinitrotoluene (TNT) [9] and glucose, the simultaneous determination of uric acid and nitrite [10], energy storage devices [11], etc. Among the various available materials, one of the most popular is carbon black/PLA (CB-PLA) conductive composite. Carbon Black is a material made of finely divided carbons produced by the thermal decomposition of a hydrocarbon. Conductive carbon particles in CBs are chemically bound and form agglomerates by weak Van der Waals interactions [12]. The conductivity of CB-PLA is dominated by percolation, which means that the addition of conductive fillers has little effect until enough filler is present to form a continuous particle pathway through the material. Recent research indicate that 3D-printed CB/PLA electrodes have promising applications as electrochemical sensors, including fuel electroanalysis [13], electrochemical cells for detection of mercury ions [14], caffeine and glucose [15], simultaneous determination of cadmium and lead ions in biological fluids [16], etc.

New carbon/polymer 3D-printout electrodes present poor electrochemical properties prior to the application of a surface activation treatment. The activation treatments remove the excess polymeric matrix to expose conductive fillers at the electrode surface. It has been well documented that the chemical activation of carbon/polymer electrodes improves the efficiency of electrochemical processes. Manzanares-Palenzuela et al. reported the surface treatment of graphene-PLA (G-PLA) by immersion in dimethylformamide (DMF) for 10 min exposed the graphene fillers [31] successfully. However, the most commonly used DMF has a negative impact on the environment. Therefore, other activation surface treatments are being investigated. One of them is electrochemical treatment in NaOH, which has highly improved the electrochemical response significantly. For example, Rocha et al. [16] studied the electron transfer after surface treatment in 0.5 mol L^{-1} NaOH by applying a constant potential of 1.4 V for 200 s and then −1.0 V for 200 s. The proposed electrochemical surface treatment by Richter et al. was used in a fully additively manufactured electrochemical sensing platform [17]. Furthermore, Browne et al. demonstrated that a combined DMF treatment and electrochemical activation process improves the activity of the 3D-printed G-PLA electrodes. Solvent treatments were performed by soaking the 3D-printed electrodes in DMF for 10 min, which was completed prior to electrochemical activation. Next, electrochemical activation of the 3D electrodes was carried out in a phosphate buffer solution (pH 7.2) using a chronoamperometry method at high oxidizing potentials for a range of times [18]. PLA, belonging to the aliphatic polyester group, is usually hydrolyzed by esterases, lipases or proteases. Acid and neutral proteases have little or no activity, but some alkaline proteases are able to form appreciable amounts of lactic acid from PLA [19]. The hydrolytic activity of enzymes depends on many factors, including pH and temperature. Successful Proteinase K-catalyzed G-PLA digestion was recently reported by Manzanares-Palenzuela et al. [20], opening a new environmentally friendly and reproducible alternative to the surface activation procedure of PLA-based 3D printed electrodes. Solvent-free activation by laser ablation was recently proposed by Glowacki et al. [21]. Further examples of post-treatment procedures for 3D-printed surfaces for electrochemical applications are presented in an interesting mini-survey by Rocha et al. [22].

This work aims to present and understand the electrochemically active surface area development of CB-PLA through controlled electrolysis, with the goal of increasing the electrode's utility as an electrochemical sensor platform.

Various polarization protocols were studied to evaluate the optimum conditions for CB-PLA activation. First, the anodic and cathodic polarization depth were evaluated for PLA electrolysis carried out in acidic and alkaline media, discussing the resultant modification to the surface chemistry and the activation mechanism. A separate study was conducted to develop the CB-PLA activation protocol by proteinase K enzymatic interaction. Finally, the efficiency of the synergistic interaction of enzymatic hydrolysis and electrolysis were reported. To the authors best knowledge, this is the first attempt to explore activation potential through both of these processes, carried out simultaneously.

2. Experimental

3D printout electrodes: Flat electrodes with the dimensions 10x10x2 mm were 3D-printed from conductive, commercially available PLA, Proto-Pasta, on an Ender 3 Pro 3D printer (Ender, China). The electrodes were horizontally printed with the parallelly-oriented layers versus the load direction. The printing temperature was 200 °C. According to the thermogravimetric analysis (presented in the **Supplementary Information file, Section S1)**, the CB-PLA filament contained 26.4 wt% carbon filler, which resulted in 30 Ωcm electric resistivity. The filament, as well as the electrodes, were stored under atmospheric conditions.

Activation protocols: The activation procedure was started immediately after the printing process. Chemical, electrochemical and enzymatic activation protocols were investigated. The electrochemical activation was carried out in acidic (1 M HCl solution, pH = 0) and alkaline (1 M NaOH solution, pH = 14) media. The activation was performed by potentiodynamic polarization scan at a constant rate of 50 mV/s for various polarization ranges. Each electrode was subjected to a total of 10 polarization cycles. The chemical and enzymatic activation treatments simply involved soaking the electrode in the target electrolyte. Solvent treatments were performed by soaking the 3D-printed electrodes in one of the studied electrolytes for 24 h. For determination of the effect of enzyme activity on the CB-PLA, two tests were performed. For the first, each 3D-printed specimen was immersed in a 0.6 mg /mL proteinase K solution prepared in a Tris-HCl buffer (Tris 100 mM, $CaCl_2$ 1 mM, pH = 8.0) and incubated at 37 °C for 24 h, 48 h, 72 h and 96 h. For the second, each 3D-printed specimen was immersed in a proteinase K solution with 0.2 mg/mL, 0.4 mg/mL, 0.6 mg/mL and 0.8 mg/mL prepared in Tris-HCl buffer (Tris 100 mM, $CaCl_2$ 1 mM, pH = 8.0) and incubated at 37 °C for 72 h. The enzyme/buffer was replaced every 24 h to restore enzymatic activity, avoiding pH value decrease. After CB-PLA electrochemical activation was finished, the samples were rinsed thoroughly with distilled water at 4 °C to stop further degradation, and then dried to achieve a constant mass. The mass loss (%) was calculated according to $(m_0 - m_t)/m_0$, where m_0 and m_t represent the dry weights of the specimens before and after degradation, respectively.

Electrochemical studies: All the electrochemical measurements, including electrochemical activation and the electrochemically active surface area (EASA) determination of the electrode, were carried out in a three-electrode setup with the 3D-printed working electrode, Ag|AgCl as the reference electrode and platinum wire as the counter electrode. The electrochemical measurements were made using a Reference 600 + potentiostat/galvanostat (Gamry Instruments, USA), controlled by Gamry Framework software.

Determination of the surface activation efficiency was based on evaluation of charge transfer kinetics in an electrolyte composed of 2.5 mM $[Fe(CN)_6]^{4-}$ and 2.5 mM $[Fe(CN)_6]^{3-}$ as the electroactive redox species dissolved in 0.5 M Na_2SO_4. Studies were performed in 5 mL electrochemical cells in naturally aerated electrolytes. Two techniques were used, namely electrochemical impedance spectroscopy (EIS) and cyclic voltammetry (CV). The EIS experiment was carried out under open circuit potential (OCP) conditions (0.25 ± 0.04 V vs Ag|AgCl), with a voltage perturbation amplitude of 10 mV, and for the frequency range of 100 000 to 0.1 Hz, 10 points per frequency decade. The CV experiments were done at a scan rate of 50 mV/s. The $[Fe(CN)_6]^{4-/3-}$ species were used as the most commonly referred redox-active probe. Moreover, the inner sphere electron transfer (ISET) mechanism of the ferrocyanides is known to be largely dependent on the electrode surface chemistry [23,24]. Thus, we found this redox probe to be particularly valuable in differentiating the efficiency of the surface activation protocols.

The standard heterogeneous rate constant k^0 was estimated from the

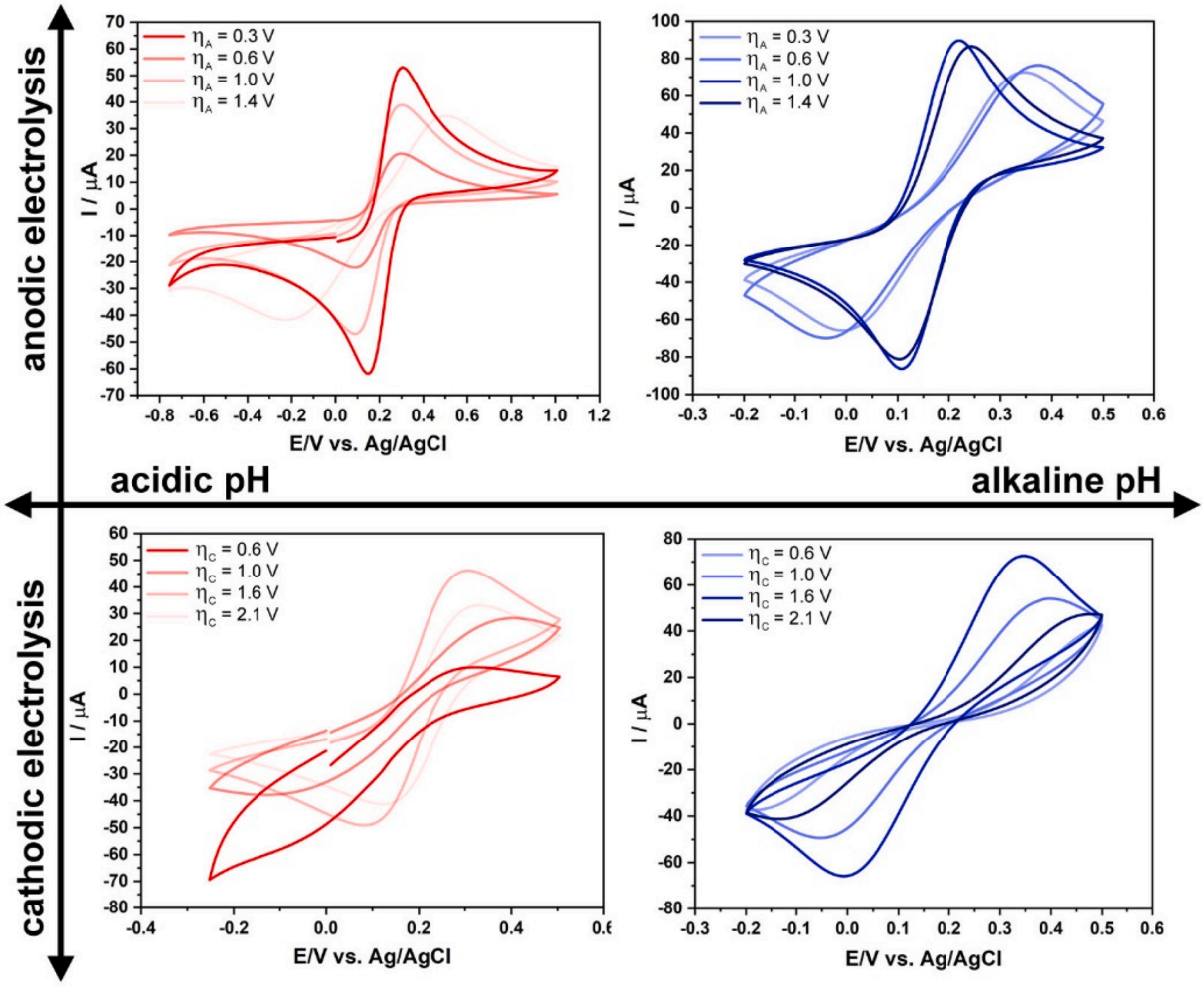

Fig. 1. a) CV curves reflecting charge transfer kinetics through the electro-activated CB-PLA electrode depending on the direction and depth of electrochemical polarization, carried out in an electrolyte with acidic (1 M HCl) and alkaline (1 M NaOH) media. Electrolyte: 0.5 M Na_2SO_4 + 5 mM $[Fe(CN)_6]^{4-/3-}$. Polarization scan rate 50 mV/s.

CV studies at a scan rate of 50 mV/s or 10 mV/s (when the electron transfer was found irreversible at higher scan rates), using the Nicholson approach, with Eq. (1) [25,26]:

$$k^0 = \psi\left(\pi D_0 \frac{nF\upsilon}{RT}\right)^{1/2} \quad (1)$$

where ψ is the dimensionless kinetic parameter estimated from the literature based on peak potential separation ΔE_P [25], D_0 is the diffusion coefficient ($6.67*10^{-6}$ cm^2/s), n is the number of electrons transferred, υ is the applied scan rate, R is the gas constant, F is the Faradaic constant and T is the temperature.

Physicochemical studies: The X-Ray photoelectron spectroscopy (XPS) studies were carried out with an Escalab 250Xi multispectroscope (Thermo Fisher Scientific, USA), equipped with a monochromatic AlKα source (spot diameter 650 µm). The high-resolution spectra of CB-PLA electrodes after various surface activation routes were collected in the core-level binding energy range of the *C 1s* and *O 1s* peaks. The pass energy was 15 eV. Charge compensation was controlled through a low-energy electron and low-energy Ar^+ flow. Next, the scanning electron microscopy (SEM) examination of the surface activated samples was carried out using an S-3400N VP-SEM microscope (Hitachi, Japan), using the secondary electron mode and 20 kV accelerating voltage. Prior to the examination, the CB-PLA electrodes were sputtered with a 10 nm gold layer.

3. Results and discussion

3.1. The CB-PLA electro-activation by PLA electrolysis

The efficiency of the electrochemical activation of each CB-PLA electrode, illustrated through CV curves, is shown in Fig. 1. The CB-PLA electrodes were subjected to potentiodynamic polarization treatment under various applied anodic (η_A) or cathodic (η_C) overpotentials, with the aim of evaluating the effect of the electrolysis on the surface electro-activation efficiency.

The results displayed in Fig. 1 confirm that the electrochemical treatment significantly enhances the charge transfer kinetics at the electrode interface, proving their successful activation, both in acidic and alkaline environments. Moreover, the charge transfer is strongly affected by the polarization direction and the polarization depth. In comparing the efficiency of the ferrocyanide/ferricyanide ion oxidation/reduction process, it should be concluded that exceptionally high efficiency is obtained by applying anodic overpotential at the electrode surface.

Ferrocyanide oxidation proceeded more efficiently at the CB-PLA electrode activated in the alkaline media than in the acidic media. The electrochemical surface area development in alkaline media was testified by the significant increase in measured redox currents (i_A = 86.3 vs 57.5 µA for alkaline vs acidic media, scan rate 50 mV/s). The charge transfer reversibility improved as well after activation in NaOH, testified

Table 1
The CV characteristics of the $[Fe(CN)_6]^{4-/3-}$ redox at the CB-PLA electrodes, obtained after various polarization treatments in 1 M HCl or 1 M NaOH electrolyte.

	1 M HCl				1 M NaOH			
η_A/V	0.3	0.6	1.0	1.4	0.3	0.6	1.0	1.4
ΔE_P/mV	443	282	192	151	356	413	112	140
i_A/μA	37.8	42.6	23.2	57.5	65.9	69.9	86.3	81.2
i_A:i_C/-	1.01	1.00	0.90	0.95	0.91	0.91	0.96	0.94
k^0/cm/s	$3.2{\cdot}10^{-4}$	$5.1{\cdot}10^{-3}$	$9.6{\cdot}10^{-4}$	$1.4{\cdot}10^{-3}$	$3.8{\cdot}10^{-4}$	$3.2{\cdot}10^{-4}$	$2.7{\cdot}10^{-3}$	$1.6{\cdot}10^{-3}$
η_C/V	0.6	1.1	1.6	2.1	0.6	1.1	1.6	2.1
ΔE_P/mV	–	390	159	180	687	447	356	615
i_A/μA	12.2	27.3	46.2	33.7	37.5	49.4	65.9	41.3
i_A:i_C/-	–	0.74	0.90	0.80	0.88	0.91	0.91	0.87
k^0/cm/s	–	$3.8{\cdot}10^{-4}$	$1.3{\cdot}10^{-3}$	$9.6{\cdot}10^{-4}$	$1.9{\cdot}10^{-4}$	$3.2{\cdot}10^{-4}$	$3.8{\cdot}10^{-4}$	$1.9e{\cdot}10^{-4}$

by $\Delta E_p = 112$ mV and i_A:$i_C = 0.96$ ($\eta_A = 1.0$ V, scan rate 50 mV/s). Given the CB-PLA activation was carried out at sufficiently high anodic polarization, the electrolysis led to higher values of k^0 and more effective redox kinetics. This effect was observable in particular at η_A exceeding 0.6 V, when the observable value of k^0 increased by an order of magnitude, peaking at 0.003 cm/s, the exact values can be found in Table 1. The considerable improvement in electron charge transfer was probably due to removing the polylactide matrix and exposing conductive CB fillers at the electrode surface. The efficiency of the activation process was more evident in alkaline media, where the oxidation peak current reached 90 μA after CB-PLA activation at the highest studied η_A. However, even when the activation was carried out at much smaller potentials, not exceeding + 0.5 V vs. Ag|AgCl, the redox process kinetics was considerable, with $i_A = 66$ μA.

The highest value of the heterogeneous rate constant k^0 after activation in acidic media was only half that, and achieved after activation at the highest anodic overpotentials applied during the activation process, with oxidation peak current i_A reaching 57.5 μA (at 50 mV/s scan rate). Nevertheless, the peak separation potential at the most efficient studied η_A was $\Delta E_P = 151$ mV, which, together with a slightly unbalanced anodic-to-cathodic current ratio i_A:$i_C = 0.95$, hints at the irreversibility of the electrochemical process. Notably, the activation performed in both studied electrolytes may lead to obtaining the quasi-reversibility regime of the redox process [27].

A key observation should also be made based on the analyses of these results. The CB-PLA electrodes should be handled with great care since the polarization regime of commonly used CV procedures when using the most popular redox probes often exceed the polarization limits sufficient for CB-PLA surface modification throughout the measurement. On the other hand, most research groups dealing with 3D printed electrodes study the electron charge transfer using potassium hexacyanoferrate(II) as the redox probe [16,18]. The impedimetric measurements may be found to be a more suitable approach to investigating the electrochemical response of 3D-printed PLA-based electrodes, which is due to the mV polarization range of the perturbation amplitude.

The polarization curves registered during the surface activation treatment are given in the **Supplementary Information file, Section S2.** The sole action of the studied electrolyte, in the absence of electrode polarization, is given in the **Supplementary Information file, Section S3.** The obtained results indicate that surface activation by PLA hydrolysis in the absence of the polarization component is also the most effective when hydrolysis in carried out in the alkaline environment, assuming a well-developed EASA and electron transfer rate. On the other hand, with very slow electron transfer kinetics of only partially-surface activated electrodes in the acidic and neutral pH environments, the obtained results were poor, without defined redox peaks. The increased PLA susceptibility to saponification in alkaline solution could be explained by more effective PLA hydrolysis under these conditions and thus better exposure of the conductive CB nanoparticles at the electrode surface. Most notably, the surface activation in 1 M NaOH under cyclic

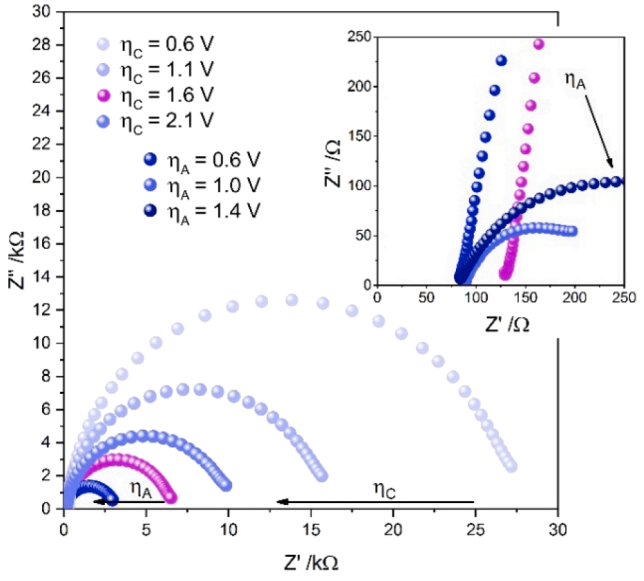

Fig. 2. EIS spectra for CB-PLA electrodes electrochemically activated under different potentiodynamic polarization conditions, in 1 M NaOH. Studies carried out in 0.5 M Na_2SO_4 + 5 mM $[Fe(CN)_6]^{4-/3-}$.

polarization conditions was found to be a time-efficient and environmentally-friendly alternative to etching in aprotic solvents such as DMF.

While anodic activation treatment leads to the pronounced CB-PLA EASA development, performing the activation process at cathodic polarization to a certain extent increases the faradaic charge transfer. However, the activation efficiency is dramatically lower, and the resultant heterogeneous rate constant barely competes with the k^0 value obtained after activation at the lower studied anodic polarization (see **Supplementary Information file, Section S4** for a graphical representation). These results prove the smaller utility of cathodic polarization treatment as a part of the 3D-printed electrode activation protocol [17,28]. Overall, the optimum electrochemical activation polarization range was determined to be from −1.4 V to +1.2 V vs. Ag/AgCl, where the smallest peak-to-peak separation and the highest redox probe faradaic current were achieved. The voltammetric EASA estimation for the optimal conditions of the electro-activation protocol is given in **Supplementary Information file, Section S5.** The obtained EASA value of 0.204 cm^2 is nearly the same as the electrolyte-exposed CB-PLA geometric surface, suggesting successful activation, where evenly distributed CB nanoparticles produce heavily overlapping diffusion layers [29].

A similar observation regarding the CB-PLA EASA development efficiency was made based on the electrochemical impedance spectroscopy measurements of the studied electrodes. These results were carried

Table 2
The electric parameters obtained for CB-PLA electro-activation in 1 M NaOH for each studied electrochemical polarization condition.

	η/V	R_{CT}/kΩ	Q/μSs^n	α/-
η_C	0.6	27.41	2.47	0.93
	1.1	15.85	4.08	0.94
	1.6	6.41	5.57	0.95
	2.1	9.92	4.97	0.93
η_A	0.3	6.41	5.57	0.95
	0.6	3.05	5.81	0.93
	1.0	0.16	43.92	0.80
	1.4	0.34	46.45	0.70

out in a 1 M NaOH solution, which was found highly effective for the activation process. The Nyquist plots are given in Fig. 2.

The impedance data were analyzed using an R(QR) electric equivalent circuit (EEC) built of a series resistance R_S (sum of the resistances of electrolyte, electrode, wires etc.) and a parallel connection of a charge transfer resistance (R_{CT}) and constant phase element (CPE) representing the electric double-layer capacitance of a heterogeneous electrode. The impedance of the CPE may be defined with Eq. (2) [30].

$$Z_{CPE} = \frac{1}{Q(j\omega)^{\alpha}} \quad (2)$$

where Q is the quasi-capacitance, j is the imaginary number, and ω is the angular frequency. For α = 1, the CPE represents the ideal capacitor, and lower α values are introduced by frequency dispersion of capacitance due to heterogeneous charge transfer at the electrode/electrolyte interface [30,31]. The electric parameters from the fitting procedure with the selected EEC are given in Table 2.

Altering the cathodic polarization potentials during the electrochemical activation of CB-PLA electrodes influences the charge transfer resistance. Compared with the previously presented untreated CB-PLA electrode (R_{CT} = 326 kΩ), the R_{CT} parameter drops by one order of magnitude yet does not fall below 6 kΩ (98% efficiency) regardless of the applied cathodic polarization depth limit. On the other hand, the deeper the anodic polarization range, the lower the R_{CT} value. In particular, for $\eta_A > 0.6$ V, the R_{CT} drops by another order of magnitude to 160.3 Ω at η_A = 1.0 V, which exceeds 99.9% activation efficiency. Notably, the EIS-measured R_{CT} characteristic of the surface-activated CB-PLA electrodes corroborates the CV-measured i_A and k^0. An interesting feature was observed when analyzing the CPE-exponent α changes, suggesting that the electric heterogeneity of each cathodically-activated CB-PLA electrode surface was similar and only decreased if the activation procedure was carried out with deep anodic polarization limits ($\eta_A > 0.6$ V). There are few possible explanations of such characteristics. Most likely, highly efficient uncovering of the conductive CB particles leads to the appearance of the surface distribution of the time-constant dispersion, falling in the mechanism of heavily overlapping diffusion layers at spatially heterogeneous electrodes [29,32]. The second plausible cause is the introduction of the normal distribution of the time constants through the appearance of the porous electrode surface.

The high-resolution XPS spectra were recorded in the *C 1s* (Fig. 3**a**) and *O 1s* (Fig. 3**b**) core-level binding energy range to determine the CB-PLA surface chemistry resulting from various electro-activation protocols and PLA etching. The untreated, 3D printed CB-PLA electrode was also studied for comparison purposes.

The polylactide chemistry includes three different carbon chemical states, namely C-C, C-O, and C = O. These three types of chemical bonds are commonly identified in the *C 1s* spectra as signals peaking at a binding energy of 284.6 eV (C2), 286.0 (C3), and 288.1 eV (C4),

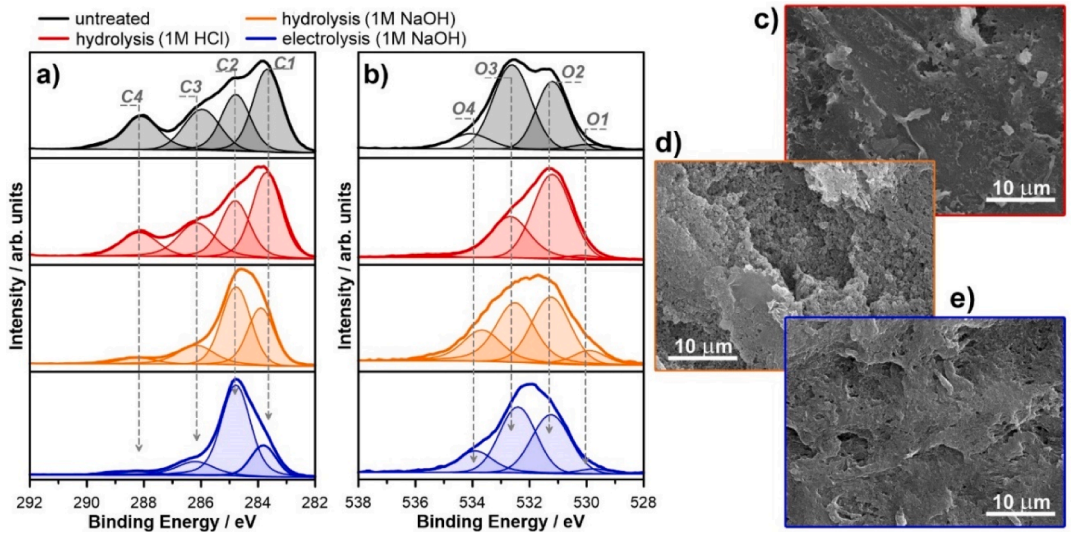

Fig. 3. a,b) XPS spectra registered in a) C 1s and b) O 1s binding energy range for the untreated CB-PLA electrode and after its electro-activation using various protocols, c-e) SEM micrographs of the CB-PLA electrode surface after hydrolysis in c) 1 M HCl and d) 1 M NaOH, and e) electrolysis in 1 M NaOH (−1.4 to +1.2 V vs. Ag|AgCl polarization range).

Table 3
The CB-PLA surface chemistry (in at.%) in terms of various chemical states of carbon and oxygen, based on XPS analysis with the deconvolution model.

		C 1s				*O 1s*			
		C1	C2	C3	C4	O1	O2	O3	O4
BE/ eV		283.7	284.6	286.0	288.1	529.9	531.2	532.7	534.1
Untreated		27.0	18.6	15.9	14.6	1.0	8.4	12.2	2.4
Hydrolysis	**HCl**	26.5	18.0	13.9	9.1	0.9	19.8	11.3	0.5
	NaOH	29.2	41.4	14.4	4.2	0.9	4.0	3.9	2.1
Electrolysis	**NaOH**	16.0	55.6	11.1	2.7	0.5	5.7	6.2	2.3

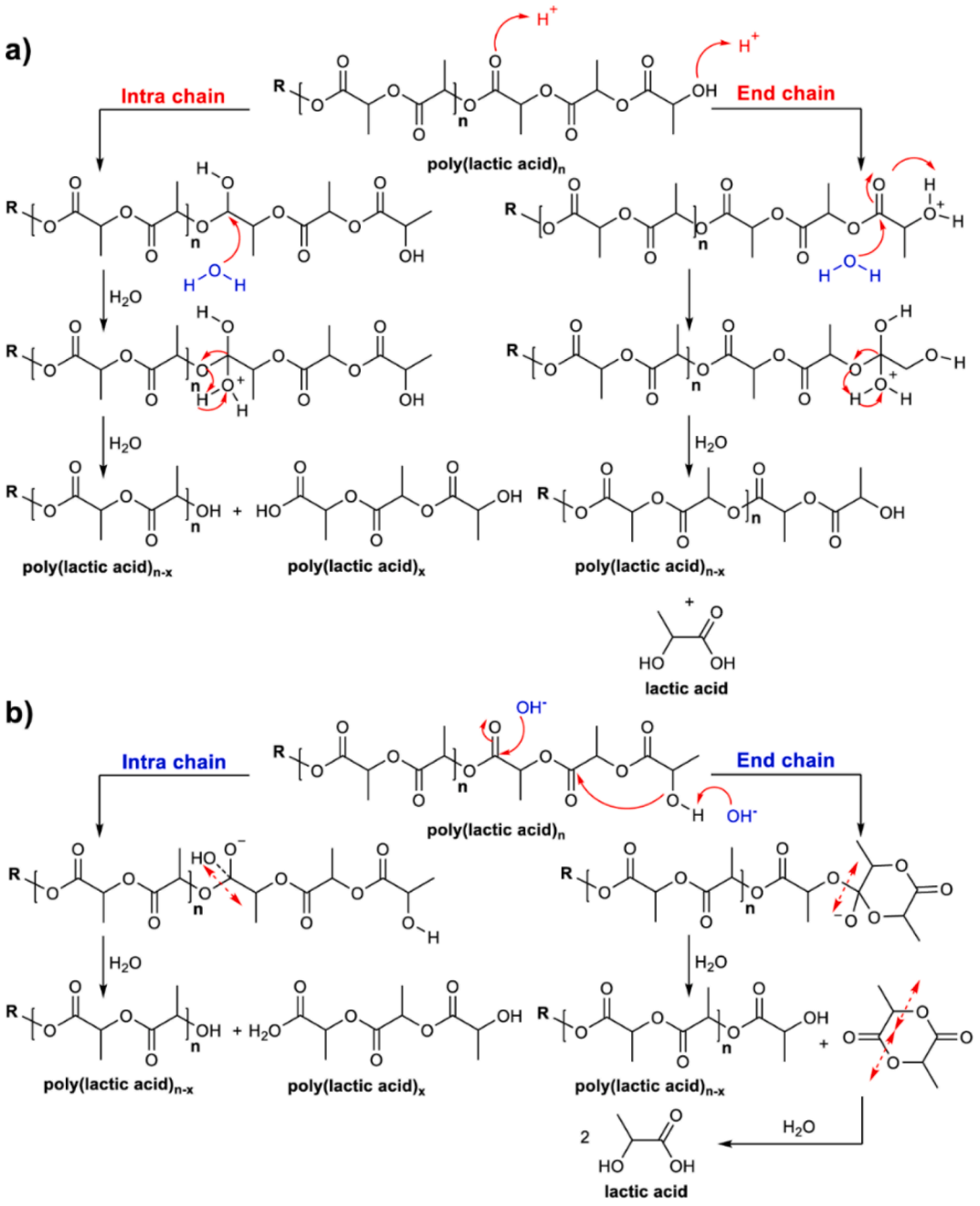

Fig. 4. The mechanism PLA hydrolysis in an a) acidic, b) alkaline environment.

respectively [21,33,34]. Furthermore, their expected ratio for PLA matrix should be 1:1:1. A similar ratio of C2:C3:C4 components was found for the untreated sample. The aliphatic C-C bonds (C2) dominated due to the simultaneous detection of surface adventitious carbon contaminants from atmospheric exposure [35]. The most prominent component (C1) recorded in the untreated PLA *C 1s* spectra lies in the energy range characteristic to the sp^2-carbon in CB [21,36,37], revealing that the approx. 27 at.% signal originates from the composite filler, corroborating the thermogravimetric analysis. The data are presented in Table 3. The oxygen chemistry analyzed for the untreated sample may also be divided to four different types of interactions. The dominant two, O2 and O3, are characteristic of C = O and C-O bonds, respectively, originating primarily from the polylactide matrix. Two minor oxygen components were also identified, first the O1 at 529.9 eV, a value typical for metal oxides, impurities to commercially available PLA filaments originating from thermal stabilizers and plasticizers [38]. Finally, oxygen in chemisorbed water molecules may result in the signal appearing at approx. 534 eV, identified as O4 [34,39].

Both carbon and oxygen chemistry are significantly affected by the applied CB-PLA surface activation protocols, yet the mechanism of the interaction based on the obtained XPS results is complex and possibly different in each case. The hydrolysis process, carried out in an aqueous 1 M hydrochloric acid solution, appears to lead to a significant increase in the share of oxygen content of 24 at.% for the untreated CB-PLA electrode up to 32.3 at.%. On the other hand, due to the PLA treatment in the alkaline environment, the amount of surface oxygen atoms is halved. This observation is visible with and without activation by electrolysis. Other XPS studies on the CB-PLA activation reveal similar effects, where a significant share of oxide groups is found for O_2 plasma compared with CO_2 [40] as well as laser ablation in air compared with a He atmosphere [21]. The above-described change is primarily recognized as the increase of C-O and C = O interactions, while the share of

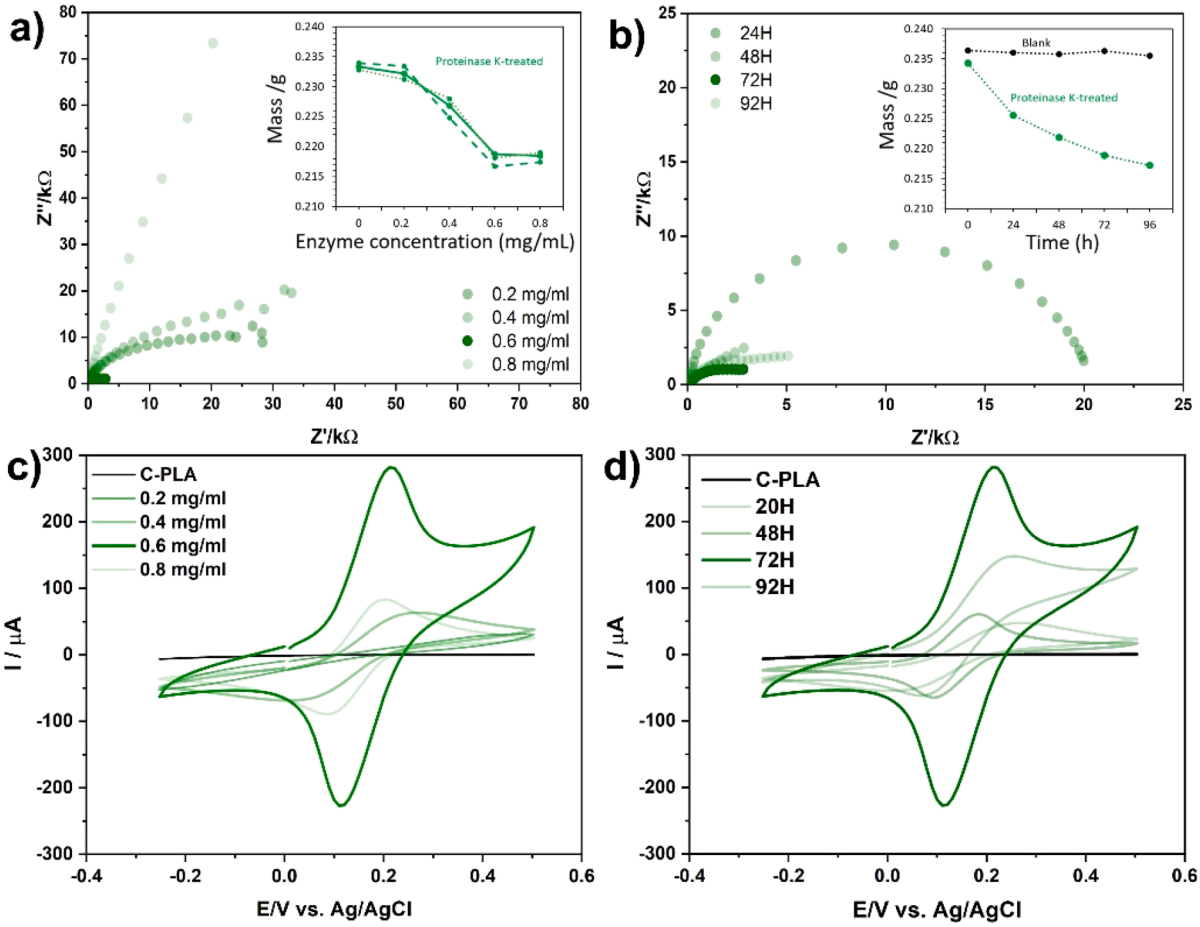

Fig. 5. a,b) CV curves and c,d) EIS spectra reflecting alteration of charge transfer kinetics, depending on various studied proteinase-K digestion conditions, i.e. a,c) enzyme concentration and b,d) enzymatic hydrolysis time. Mass variation during CB-PLA electro-activation in the inset: a) 72 h activation, b) 0.6 mg/mL proteinase-K concentration.

O1 and O4 components is negligibly affected by the chemical oxidation process and does not exceed 1.4 and 2.4 at.%, respectively. This effect will be discussed later.

The exposure of the electrically conductive carbon black filler at the CB-PLA surface is evident based on the increase in charge transfer kinetics through the activated electrode. However, this observation is not confirmed by the rise in *C 1s* carbon black nanofiller C1 component share. This is an important yet unexpected observation, confirmed by each studied activation procedure, either through PLA hydrolysis or electrolysis. One possible explanation of this mechanism may originate from partial oxidation of the sp^2-carbon filler material. The excessive oxidation of the electrode surface during the electrolysis process was presumably the cause of the more irreversible charge transfers observed after anodic electrochemical activation of 3D printed CB-PLA electrodes by Vaněčková et al. [41]. According to this hypothesis, the amount of CB exposed at the electrode surface increases, yet its oxidation leads to a positive binding energy shift towards energies characteristic for the C2 or even C3 components, superimposing with the PLA-based features. A possible confirmation of the above-presented explanation may be found in our recent XPS examination of the surface PLA treatment by laser ablation in an air and helium atmosphere, leading to CB-PLA electrochemical activation. Laser ablation in an air atmosphere is characterized by a nearly 25% decrease of C1 with a similar increase in C2 peak share. On the other hand, the noble gas matrix does not lead to CB oxidation, resulting in an over 20% C1 increase and only a 7% C2 increase compared with the results of the untreated CB-PLA electrode [21].

An optional explanation of the above phenomenon is the rapid surface area development of the CB-PLA electrode due to PLA hydrolysis process, leading to breaking of the ester bond and an increase in the amount of aliphatic C-C bonds at the surface, confirmed by a rapid decrease of C = O bonds (C4, O2 peaks), in particular in an alkaline environment. The development of the surface area will also result in an increased amount of surface-adsorbed adventitious carbons. Surface area development is visible on SEM micrographs, see Fig. 3**c-e**. A possible mechanism for the PLA hydrolysis is presented in Fig. 4. The decrease in C1 share may also be attributed to the detaching of loosely linked conductive carbon nanoparticles by PLA hydrolysis or a binding energy shift resulting from the disappearance of C-C bonds between the CB and the polymer [42]. Notably, the above-proposed hypotheses do not exclude each other, and both may co-occur, although verification requires independent studies.

The hydrolysis of the PLLA (poly(L-lactic acid) ester bonds occurs in acidic and alkaline environments. It is well known that the hydrolytic degradation of ester bonds is slow in aqueous conditions, while it is much faster in alkaline environments than in acidic ones [43]. The efficiency of PLLA hydrolysis is very slow in neutral pH and moderate acidic and alkaline solutions. Therefore, the activation of the CB-PLA surface was performed in strongly acidic (pH = 0) and alkaline (pH = 14) media, with the hydrolytic degradation being much faster in the latter. The mechanism of PLA hydrolysis previously proposed by Lucas et al. [44] involves two paths of degradation by intrachain or end chain of the PLA regardless of the environment.

The mechanism of PLA hydrolysis performed in an acidic solution involves the protonation of the hydroxyl groups end groups, which leads to the formation of intramolecular hydrogen bonds and contributes to the hydrolysis reaction and the formation of free lactic acid, causing the

Table 4
CV characteristics of the $[Fe(CN)_6]^{4-/3-}$ redox at the CB-PLA electrodes, obtained at various proteinase K digestion conditions, measured at polarization at a scan rate of 50 mV/s.

	Concentration/mg/mL				Activation time/h			
η_A/V	0.2	0.4	0.6	0.8	20	48	72	92
ΔE_P/mV	–	201	91	111	221	250	91	141
i_A/μA	–	54.5	222.4	87.0	44.4	60.2	222.4	80.9
i_A:i_C/-	–	1.04	0.96	1.04	1.06	1.01	0.96	1.00
k^0/cm/s	–	$7.7{\cdot}10^{-4}$	$4.8{\cdot}10^{-3}$	$2.9{\cdot}10^{-3}$	$5.8{\cdot}10^{-4}$	$5.4{\cdot}10^{-4}$	$4.8{\cdot}10^{-3}$	$1.6{\cdot}10^{-3}$

decrease in length of PLA. On the other hand, the acidic conditions lead to the random protonation of the carbonyl group and the PLA oxygen leads to the intramolecular hydrolysis of the ester bonds in the PLA chain. This reaction causes the degradation of the polymer and the formation of PLA chains consisting of lower molecular weights (Fig. 4a). The hydrolytic degradation of PLA also occurs in a strongly alkaline solution, where it involves intramolecular degradation and a reaction at the polymer end groups. One possible mechanism of end chain PLA degradation, including intramolecular transesterification, is suggested by Jong [45] (Fig. 4b). In alkaline conditions, the nucleophilic attack of the hydroxyl end group on the carbonyl group causes the formation of a six-membered ring as an intermediate. The newly formed free lactide hydrolyzes into two species of lactic acid. However, the intramolecular chain is randomly hydrolyzed as a hydroxide ion attacks the carbonyl groups of esters leading to hydrolysis. In this reaction path, two new molecules are formed.

The results of the XPS studies confirm that during the electrochemical degradation in an acidic solution, the significant increase in the share of oxygen content, from approx. 24 at.% for the untreated CB-PLA electrode up to 32.3 at.% can be observed, which can be a consequence of both the intramolecular hydrolysis and hydrolysis occurring at the end groups. Furthermore, the hydrolysis performed in an alkaline solution causes the share of surface oxygen atoms to be half that, which suggests that intramolecular hydrolysis is preferred.

The alteration of the electrode polarization causes the alkalization of the electrode surface in the anode area and acidification in the cathode area. Additionally, the solution pH has a significant influence on the alkalization or acidification at the electrode surface. The total effect, dependent on the implementation of electrochemical process conditions, can lead to a local pH change towards effective acidic or alkaline hydrolysis of PLA. Therefore, the overall efficiency depends on the sum of both overlapping processes. Thus, the applied polarization significantly influences the PLA hydrolysis, as shown in Fig. 1.

3.2. CB-PLA electro-activation by synergistic electrolysis and enzymatic hydrolysis interaction

Proteinase K is an enzyme used to catalyze the hydrolysis of PLLA (poly(L-lactic acid) since the structure of the PLLA monomer is similar to alanine [46]. The hydrolytic activity of enzymes depends on many factors, including pH and temperature. The critical parameter is also the chirality of the lactide unit, which exists in three diastereoisomeric forms: L-lactide (PLLA), D-lactide (PDLA) and meso-lactide [47]. Both PLLA and PDLA are enzymatically hydrolyzed by two different classes of enzymes: proteases and lipases. One of the best known efficiently hydrolyzing PLA alkaline proteases is proteinase K. A successful Proteinase K-catalyzed G-PLA digestion was recently reported by Manzanares-Palenzuela et al. [20], opening a new environmentally friendly and reproducible alternative for the surface activation procedure of PLA-based 3D printed electrodes. These significant studies indicate the possibility of CB-PLA activation through enzymatic hydrolysis; however, the prolonged treatment duration hinders the potential laboratory applications of this approach.

Due to the reported long time required for enzymatic hydrolysis, we have decided to verify the possibility of achieving the synergistic interaction between enzymatic and electrochemical PLA surface activation for a more time-efficient protocol. In order to do so, first we studied the enzymatic-driven surface activation of the carbon black-PLA electrodes, achieving tailorable electrode performance, dependent on the Proteinase K digestion conditions. The results of the enzymatic hydrolysis on the CB-PLA electrode are summarized in Fig. 5.

Increasing the proteinase K concentration from 0.2 mg/mL to 0.6 mg/mL improved the electrode surface activation effect. The peak separation of the ferrocyanide redox probe was reported as 91 mV at 0.6 mg/mL proteinase K concentration, allowing the estimation of the heterogeneous rate constant k^0 at 0.05 cm/s, almost twice the value obtained previously, in the case of the most effective electrochemical activation protocol. Likewise, the faradaic oxidation currents i_A significantly exceeded the CB-PLA values after the electrochemical activation protocol (86.3 μA), reaching 222 μA (at 50 mV/s scan rate) for a proteinase K concentration of 0.6 mg/mL. These parameters are reported in Table 4. However, at higher concentrations (0.8 mg/mL), the reaction will no longer speed up since the amount of substrate was available at all the enzyme active sites at the electrode surface, reaching the rate-limiting factor. Thus, the optimal concentration of the enzyme in the tested system was 0.6 mg/mL. Increasing the enzyme concentration will speed up the reaction. However, once all substrates are bound, the reaction will no longer speed up since there will be nothing on which the enzymes may bind [48].

The CV studies find confirmation in the shape of the impedimetric spectra. At the lowest proteinase K concentration, the R_{CT} exceeded 300 kΩ and dropped significantly, with the enzyme concentration increase reaching 20.3 kΩ at 0.6 mg/mL. However, the shape of the impedance spectra after enzymatic activation was more complex than previously reported for electrochemical treatment, revealing a second time-constant most likely originating from the surface-adsorbed proteinase K layer. These results corroborate the mass loss measurement presented in the inset of Fig. 5**a**, where the maximum mass loss of about 170 mg after 72 h exposure was consistently reported after digestion in a 0.6 mg/mL proteinase K concentration, with the plateau observable as a result of PLA digestion at higher enzyme concentrations.

The CB-PLA mass-loss studies after enzymatic action in Fig. 5**d** reveal the PLA digestion rate over the exposure duration. Notably, the highest mass loss was observed during the first day of activation and then slowly reaching a plateau at higher exposure times. Nevertheless, even after 72 h of exposure, further digestion is still observable. This result provides another proof of different 3D printed PLA-based electrode surface activations by proteinase K depending on the conductive carbon filler since in the original studies the longer digestion times (72 h) disintegrated the 3D-printed electrodes [49]. In the case of CB-PLA, no such behavior was observed. On the contrary, the highest surface activation efficiency measured with the heterogeneous rate constant k^0 and faradaic oxidation current i_A values was incomparably smaller in the case of smaller activation durations.

The short, one-day-long activation procedure as reported by Manzanares-Palenzuela et al. [49] was found of little efficiency in the case of CB-PLA. Even at 72 h exposure, the reported proteinase K concentration of 0.2 mg/mL was insufficient to reveal the faradaic currents originating from the redox probe, suggesting that the CB-PLA composite shows significantly lower activation efficiency than the originally used

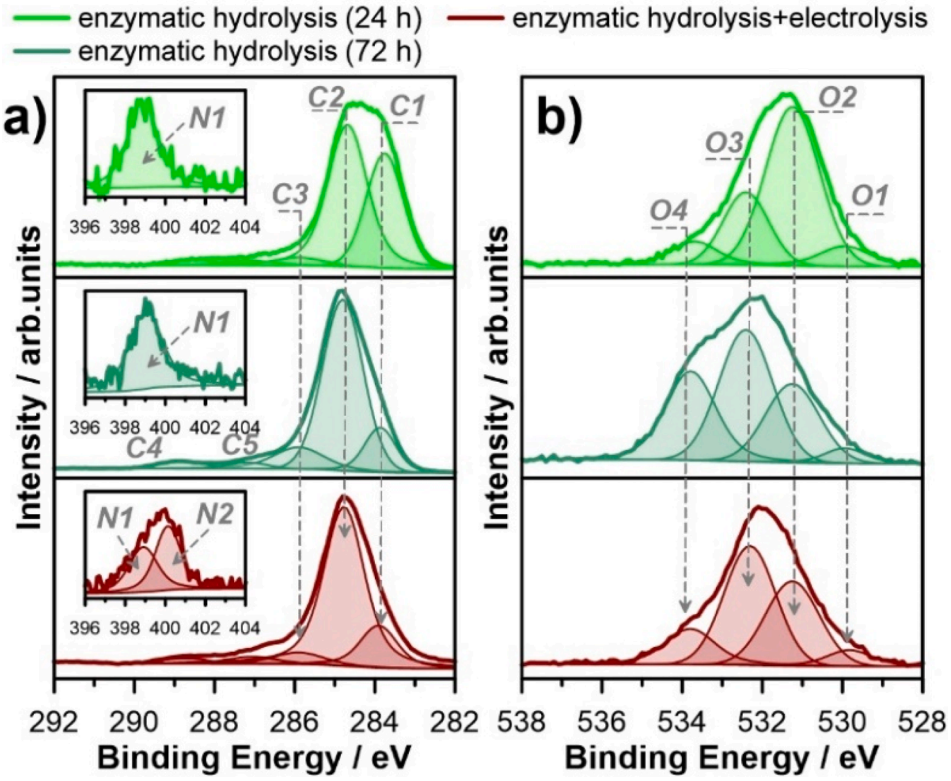

Fig. 6. XPS spectra registered in a) C 1s and b) O 1s binding energy range for the CB-PLA electrode after activation in proteinase K for 24 and 72 h, and after the combined action of electrolysis (−1.4 to +1.2 V vs Ag|AgCl polarization range) and enzymatic hydrolysis. The N 1s spectra in the inset.

Table 5
The CB-PLA surface chemistry (in at.%) after enzymatic hydrolysis in terms of various chemical states of carbon, oxygen and nitrogen, based on the XPS analysis with the deconvolution model.

		C 1s					*O 1s*			*N 1s*		
		C1	**C2**	**C3**	**C5**	**C4**	**O1**	**O2**	**O3**	**O4**	**N1**	**N2**
BE/ eV		283.7	284.6	286.0	287.2	288.5	529.9	531.2	532.7	533.8	399.0	400.1
Enzymatic hydrolysis	**24 h**	31.8	43.5	6.0	2.2	1.8	1.1	7.8	3.0	1.2	1.5	–
	72 h	14.0	62.1	9.3	2.1	2.8	0.4	2.2	3.6	2.5	1.1	–
Synergistic action		14.1	57.9	5.4	3.2	1.9	0.9	4.8	6.5	2.2	1.4	1.7

G-PLA. The proteinase K-catalyzed degradation rate is determined by the type, concentration, shape, dimension, dispersion, and adhesion of the fillers [50]. For example, fullerene and carbon nanotubes accelerated the enzymatic degradation due to the creation of large gaps between the PLA phase and facilitation of the proteinase K diffusion into the material (inside and surface cleaving). Because of the lack of adhesiveness of the fillers mentioned above to the PLA phase, they should have been readily released from the film surface, forming a porous structure increasing the surface area for the action of the enzyme (facile release). They also confirmed that conventional carbons have minimal effects on the enzymatic degradation rate [50]. Thus, carbon black probably forms small gaps in the PLA matrix and releases poorly from its surface.

The XPS analysis (Fig. 6) reveals the progressive digestion of the PLA by the proteinase K. One can notice that enzymatic hydrolysis duration leads to the decreased share of the CB NP's (C1 component), reaching 14 at.% at the end of a 72 h digestion process, a similar trend to the one presented for the most efficient alkaline electrolysis experiment. This effect is assisted by a significantly decreased share of the oxidized carbon bonds, C-O (C3, O3), C = O (C4, O2). Moreover, the exposition to proteinase K leads to a small share of C-N bonds at the electrode surface, labeled as C 1s C5 peak at 287.2 eV and N 1s N1 peak at 399.0 eV. These peaks were ascribed to sp^2 hybridized N bonded to three atoms, C-N(-C)-C or C-N(-H)-C [51,52]. The total share of these species based on the C5 + N1 sum peaks at 3.5 at.% and is independent of the studied proteinase K digestion duration. It was confirmed that the enzymatic action does not lead to excessive surface oxidation as the combined share of C3, C4, C5, O2, O3 peaks does not exceed 21 at.% compared to 26 at.% for activation in alkaline media (either through electrolysis or hydrolysis) and over 54 at.% for hydrolysis in acidic media. Thus, it is most plausible that the rapid increase in C2 peak share after successful surface activation is due to the surface area development rather than conductive carbon oxidation. The complete XPS analysis is summarized in Table 5.

The primary mechanism of proteinase K digesting of PLA polymer involves the use of a nucleophilic residue to cleave an ester bond. Serine proteases use an active serine to perform a nucleophilic attack on carbon of the ester group. Proteinase K degraded the amorphous and homo crystalline regions of PLA films to produce oligo(lactic acid)s consisting mainly of linear ones and including small amounts of cyclic forms [53,54]. The enzymatic degradation mechanism depends on the enzyme's ability to recognize protein homologs, e.g. the lactic acid analogy in PLLA polymer to the L-alanine abundant in silk fibroins. Moreover, it is known that proteases can hydrolyze n-butyl or ethyl-D- and L-lactate but cannot PDLA, which is probably due to the problem with PDLA

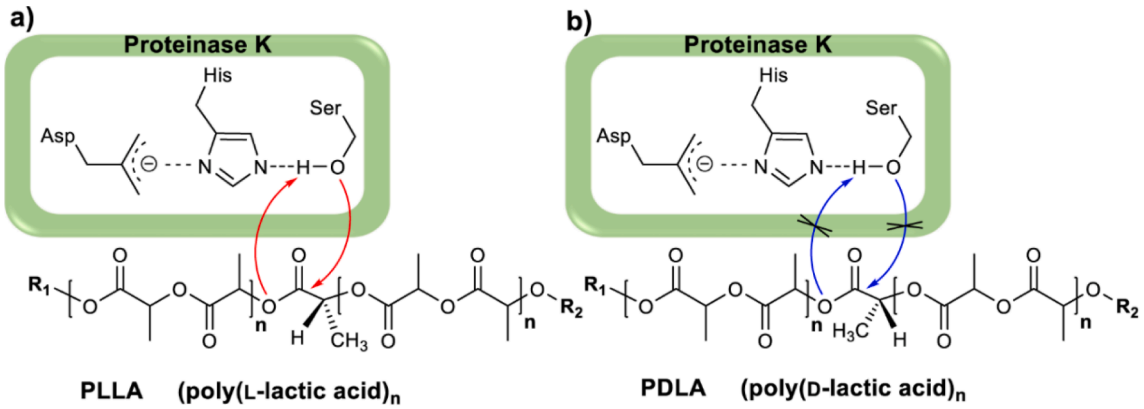

Fig. 7. The mechanism of Proteinase K action in the presence of a) PLLA and b) PDLA.

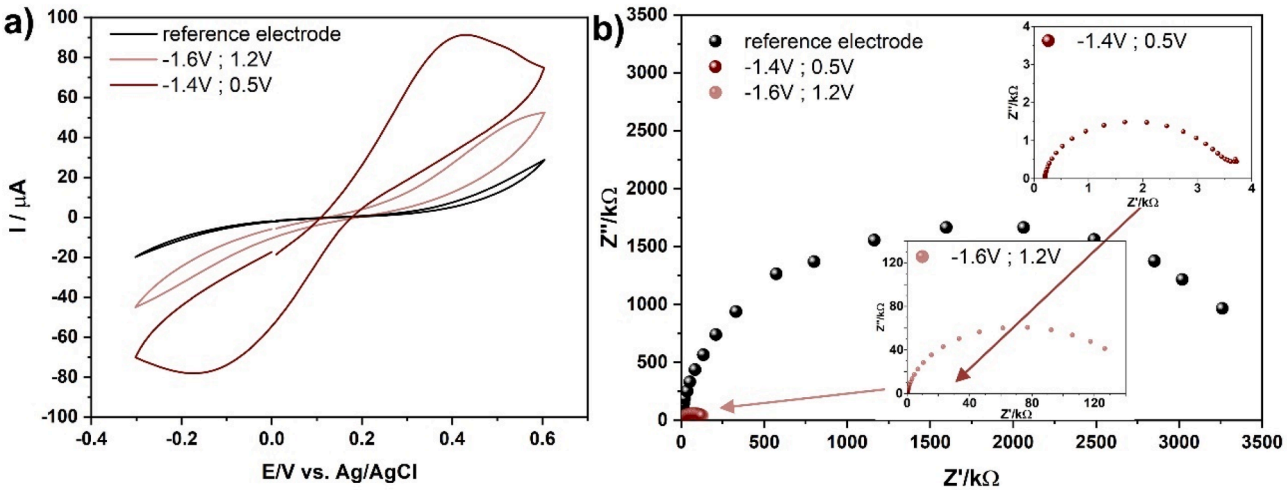

Fig. 8. The results obtained for the CB-PLA electrode subjected to electrolysis in the presence of proteinase K: a) CV curves (50 mV/s scan rate) and b) EIS spectra reflecting the charge transfer at the CB-PLA electrode for the narrow and wide polarization ranges.

accommodation in the active site or making an acyl-enzyme intermediate. In PLLA the free electron pair present on the serine oxygen can interact with the carbon of the ester group and induce digestion. In the PDLA isomer, the methyl group creates a steric hindrance that blocks the substrate from accessing the enzyme's active site [55].

The proposed mechanism was previously described by Kawai [36] and lead to the random cleavage of ester bonds in PLLA in a relatively short time (Fig. 7**a**), while this process is not observed in the presence of PDLA (Fig. 7**b**). Proteinase K is a serine protease with the classic catalytic triad of Asp^{39}-His^{69}-Ser^{224} at its active site [56]. In the presented mechanism (Ser) is the primary nucleophile, while (His) plays a dual role both as a proton acceptor and donor at different steps in the reaction. The primary function of (Asp) is based on bringing the (His) residue to the correct orientation to facilitate nucleophilic attack by (Ser) [57]. The lack of hydrolysis observed in the PDLA results from the stereochemistry mismatch of the catalytic triad and PDLA (poly(D-lactic acid) or the impossibility of making an acyl-enzyme intermediate.

The prolonged activation duration of CB-PLA electrodes under proteinase K digestion is unattractive when considering the effective use of this activation protocol in laboratory studies. Therefore, we have verified the applicability of an electrochemically-catalyzed enzymatic action to shorten the activation duration. Due to their chemical structure, enzymes are proteins. Like other proteins, they are endowed with a net charge, which is determined by the quantitative and qualitative composition of amino acids in the primary structure, spatial arrangement in the higher-order structures, and the conditions of the environment in which they are located. The action of an electric field in an enzyme solution may cause the conformational change of the active site, the inhibition of the binding of substrate to protein, and the destabilization of the protein structure, which ultimately decreases the protein's activity [58].

The synergistic action of enzymatic hydrolysis and electrolysis on CB-PLA etching was studied at an elevated temperature (37 °C) and in Tris-HCl buffer (pH = 8), necessary for successful enzyme incubation. The results of this treatment are shown in Fig. 8. In addition, the effect of the electrochemical CB-PLA activation in Tris-HCl buffer at room temperature and at 37 °C was studied, and the results presented in the **Supplementary Information file, Section S6**. In the absence of proteinase K, the electrolysis process gave sub-optimal surface activation efficiency, with barely distinguishable redox processes and a negligible effect of temperature increase.

The enzymatic hydrolysis under the previously optimized polarization regime negligibly affected the very poor CB-PLA electrode kinetics. Although the nonlinear Butler-Volmer characteristics were now observable in the CV studied polarization range, the redox probe process was still indistinguishable, assisted by a decrease in the charge transfer resistance to approx. 150 kΩ. Oxidation and reduction peaks appear on the potentiodynamic polarization scan during the activation process (**Supplementary Information file, Fig. S7a**). The reduction peak at −1.2 V vs. Ag|AgCl may be explained by immobilizing the proteinase K on the CB-PLA surface [59]. In contrast, the surface modification is oxidized at +0.9 V. Since the process is irreversible, the corresponding

Table 6
Optimized CV characteristics of the CB-PLA electrodes after various applied activation protocols.

Filament	Activation protocol	Redox probe	ΔE_p/mV	R_{CT}/Ω	k^0/cm/s	Ref.
CNT-PLA CB-PLA	Electrochemical activation CV: −0.1 V and + 3.1 V in PBS (DMF treated)	4 mM $[Fe(CN)_6]^{4-}$ in 0.5 M KCl	251	n/a	$5.0{\cdot}10^{-4}$	[60]
G-PLA	Electrochemical activation +1.8 V in 0.1 M PBS (pH 7.4) and 1 M NaOH	5 mM $[Ru(NH_3)_6]^{3+}$ in 0.1 M KCl	115	280	$1.5{\cdot}10^{-3}$	[28]
CB-PLA	Electrochemical, 1 M NaOH CV: −1.4 ÷ +1.2 V	5 mM $[Fe(CN)_6]^{4-/3-}$ in 0.5 M Na_2SO_4	112	160	$2.7{\cdot}10^{-3}$	This work
CB-PLA	Polishing + electrochemical in 0.5 M NaOH; CV ± 1.2 V	2 mM $[Fe(CN)_6]^{4-}$ in 0.1 M KCl	150*	2050	n/a	[61]
CB-PLA	Polishing + electrochemical in 0.5 M NaOH: +1.4 and −1.0 V (200 s each)	1 mM $[Fe(CN)_6]^{4-}$ in 0.1 M KCl	297	n/a	$8.3{\cdot}10^{-3}$	[16]
CB-PLA	Polishing + electrochemical in 0.5 M NaOH: 1. + 1.4 V for 200 s 2. −1.0 V for 200 s	1 mM $[Ru(NH_3)_6]^{3+}$ in 0.1 M PBS and 1 M KCl	1. n/a 2. 150*	n/a	$9.9{\cdot}10^{-3}$	[17]
CB-PLA	Electrochemical, 1 M HCl CV: −1.4 ÷ +1.2 V	5 mM $[Fe(CN)_6]^{4-/3-}$ in 0.5 M Na_2SO_4	151	n/a	$1.4{\cdot}10^{-3}$	This work
G-PLA	Enzymatic in proteinase K	1 mM $[Fe(CN)_6]^{4-}$ in 0.1 M KCl	350	n/a	n/a	[20]
CB-PLA	Enzymatic, 72 h, proteinase K (0.6 mg/mL)	5 mM $[Fe(CN)_6]^{4-/3-}$ in 0.5 M Na_2SO_4	91	~2300	$4.8{\cdot}10^{-3}$	This work
CB-PLA	Electrografting, proteinase K (0.6 mg/mL), CV: −1.6 ÷ +0.5 V	5 mM $[Fe(CN)_6]^{4-}$ in 0.5 M Na_2SO_4	632	~3500	$4.0{\cdot}10^{-5}$	This work
CB-PLA	Laser ablation in: 1. He, 2. air	1 mM $[Ru(NH_3)_6]^{3+}$ in 0.1 M KCl	1. 161 2. 141	1. 250* 2. 285*	1. $2.8{\cdot}10^{-3}$ 2. $2.4{\cdot}10^{-3}$	[21]
CB-PLA	Plasma-treated in: 1. CO_2 2. O_2	1 mM $[Fe(CN)_6]^{4-}$ in 0.1 M KCl	1. 301 2. 156	1. 1915 2. 394	1. $4.1{\cdot}10^{-4}$ 2. $2.0{\cdot}10^{-3}$	[40]
G-PLA	Annealing in vacuum at 350 °C (3 h, N_2)	10 mM $[Fe(CN)_6]^{4-}$ in 1 M KCl	255	11.1	$1.7{\cdot}10^{-4}$	[62]

*Data estimated from the plots in the articles. The authors did not provide exact values

faradaic currents develop with consecutive polarization scans.

A second experimental approach was carried out in a narrower potentiodynamic polarization range with the anodic overpotentials not exceeding the value of the anodic polarization peak (CV scans upon η_A = 0.3 V, seen in the **Supplementary Information file, Fig. S7b**) to avoid removal of the proteinase K-functionalized layer. Performing the polarization in these conditions allowed us to observe prominent oxidation/reduction peaks from the ferrocyanide redox probe. The measured ΔE_P = 632 mV (scan rate 50 mV/s) hints at the irreversibility of the electrochemical process with the heterogeneous rate constant of approximately $4.0{*}10^{-5}$ cm/s. Nevertheless, the irreversible electrode kinetics and the electrochemically active surface area (EASA) by carbon black is well-developed under proteinase K digestion with electrolysis co-occurrence. The direct proof of significant EASA development is the high value of the oxidation faradaic current i_A, exceeding 90 μA at the studied scan rate, similar to surface activation in 1 M NaOH electrolyte. The charge transfer resistance measured in the optimized enzymatic-electrochemical activation conditions was not less than 3.5 kΩ. The conclusion should be drawn, attributing the enhancement of the ferrocyanide kinetics and CB-PLA EASA development to the surface modification during proteinase K electrografting [59].

The XPS analysis was carried out to study the surface chemistry of the sample after the combined enzymatic hydrolysis and electrolysis (η_A = 0.3 V). The surface carbon chemistry revealed a high resemblance to the previously studied electrodes after enzymatic hydrolysis (72 h) and alkaline electrolysis due to the similar electrochemical surface area development level, as testified by the electrochemical EASA examination. The essential differences observed were the decreased share of the C-O bonds (C3 drops by a factor of two, down to 5.4 at.%) and an increased amount of C-N species (C5 + N1 increased by half, reaching 4.6 at.%). Moreover, another form of nitrogen appeared, N2, peaking at 400.1 eV, attributed to hydrogen-bonded/protonated NH_2/NH_3^+ amine species [51]. The total nitrogen share grew twice. All the above observations hint at the electrodeposition by proteinase K.

The studies carried out on the combined enzymatic and electrolysis action towards the increase of CB-PLA electrochemical activation confirm the simultaneous activation of the CB-PLA electrodes vυ and that this modification route may be a new and invaluable direction of enhancing enzyme activity, which requires a separate research path.

4. Final remarks

The CB-PLA electrolysis by potentiodynamic polarization is the most efficient when carried out in an alkaline environment, delivering higher EASA and an improved electron transfer rate. In particular, for anodic overpotentials reaching η_A = 1.2 V the oxidation peak current i_A of 86.3 μA (at 50 mV/s scan rate) and the peak-to-peak separation of ΔE_P = 112 mV were recorded. At the same time, the surface chemistry analysis by XPS revealed a significant decrease in oxygen content down to 12% when compared with the untreated surface (32.3 at.%). However, the surface activation is less affected when the cathodic polarization range is modified, with the most efficient activation achieved at η_C = 1.6 V. The solution pH significantly influences the alkalization or acidification of the electrode surface, which is further enhanced by changes in electrode polarization. The total effect, dependent on the implementation of electrochemical process conditions, can lead to a local pH change towards effective acidic or alkaline hydrolysis of PLA. The hydrolytic decomposition mechanism of PLA in strong alkaline conditions was attributed to the end chain degradation by intramolecular transesterification.

The enzymatic hydrolysis by proteinase K is less efficient for CB-PLA than in the case of the previously reported G-PLA composite. The difference most likely originates from small gaps between the CB and PLA phases, hindering proteinase K diffusion. The optimized digestion conditions were as follows: 72 h exposure at a 0.6 mg/mL proteinase K concentration, which resulted in very high ferrocyanide oxidation currents, i_A = 222 μA, and higher reversibility (ΔE_P = 91 mV). Our results suggest enzymatic hydrolysis to be a significantly more effective protocol for CB-PLA electrochemical activation than electrolysis in either 1 M NaOH or 1 M HCl. However, prolonged treatment duration hinders potential laboratory applications of this approach.

Finally, we have demonstrated the novel strategy of electro-

activation of 3D-printed carbon black/poly(lactic acid) electrodes based on simultaneous surface treatment by electrolysis and enzymatic hydrolysis with proteinase K. This allows a unique synergistic interaction for tailoring of electrolysis and enzymatic hydrolysis, both for the electrochemically active surface area and electron transfer kinetics. This activation protocol has led to EASA development comparable to alkaline electrolysis activation (i_A = 90 μA), yet providing irreversible electron transfer kinetics. Furthermore, the XPS analysis reveals a high resemblance of the CB-PLA electrodes after enzymatic hydrolysis (72 h) and alkaline electrolysis, thanks to the analogous electrochemical surface areas. The enhanced charge transfer kinetics were attributed to proteinase K electro-polymerization under the cathodic currents. It should be noted that the electro-polymerization introduces surface modification rather than just uncovering conductive CB particles, as in the case of other protocols.

The optimized values of the electrochemical parameters obtained for each studied activation protocol together with recent literature findings for various electro-activation protocols were summarized in Table 6.

It may be concluded that the lowest ΔE_P and highly competitive k^0 values were found for our CB-PLA electrode activated by enzymatic hydrolysis in proteinase K, with time- and cost-efficient electrolysis in 1 M NaOH being only slightly inferior.

CRediT authorship contribution statement

Adrian Koterwa: Investigation, Writing – original draft, Visualization, Data curation. **Iwona Kaczmarzyk:** Investigation, Writing – original draft, Visualization, Data curation. **Szymon Mania:** Investigation, Writing – original draft, Methodology. **Mateusz Cieslik:** Investigation, Writing – original draft. **Robert Tylingo:** Writing – review & editing. **Tadeusz Ossowski:** Writing – review & editing. **Robert Bogdanowicz:** Writing – review & editing, Funding acquisition. **Paweł Niedziałkowski:** Writing – original draft, Writing – review & editing, Conceptualization. **Jacek Ryl:** Investigation, Writing – original draft, Writing – review & editing, Conceptualization, Methodology, Funding acquisition, Visualization.

Declaration of Competing Interest

The authors declare that they have no known competing financial interests or personal relationships that could have appeared to influence the work reported in this paper.

Acknowledgements

This work was supported by The National Science Centre (Republic of Poland) under project SONATA BIS number 2020/38/E/ST8/00409 and by The National Centre of Research and Development (Republic of Poland) under project POLNOR number NOR/POLNOR/UPTURN/0060/2019-00.

Appendix A. Supplementary data

Supplementary data to this article can be found online at https://doi.org/10.1016/j.apsusc.2021.151587.

References

[1] T. Han, S. Kundu, A. Nag, Y. Xu, 3D printed sensors for biomedical applications: a review, Sensors 19 (2019) 1706, https://doi.org/10.3390/s19071706.
[2] M.D. Symes, P.J. Kitson, J. Yan, C.J. Richmond, G.J.T. Cooper, R.W. Bowman, T. Vilbrandt, L. Cronin, Integrated 3D-printed reactionware for chemical synthesis and analysis, Nat. Chem. 4 (5) (2012) 349–354, https://doi.org/10.1038/nchem.1313.
[3] A. Melocchi, F. Parietti, A. Maroni, A. Foppoli, A. Gazzaniga, L. Zema, Hot-melt extruded filaments based on pharmaceutical grade polymers for 3D printing by fused deposition modeling, Int. J. Pharm. 509 (1-2) (2016) 255–263, https://doi.org/10.1016/j.ijpharm.2016.05.036.
[4] M. Wang, P. Favi, X. Cheng, N.H. Golshan, K.S. Ziemer, M. Keidar, T.J. Webster, Cold atmospheric plasma (CAP) surface nanomodified 3D printed polylactic acid (PLA) scaffolds for bone regeneration, Acta Biomater. 46 (2016) 256–265, https://doi.org/10.1016/j.actbio.2016.09.030.
[5] L. Xiao, B. Wang, G. Yang, M. Gauthier, Poly(Lactic Acid)-Based Biomaterials: Synthesis, Modification and Applications, in: D.N. Ghista (Ed.), Biomedical Science, Engineering and Technology, InTech, 2012. https://doi.org/10.5772/23927.
[6] D. Garlotta, A literature review of poly(lactic acid), J. Polym. Environ. 9 (2001) 63–84, https://doi.org/10.1023/A:1020200822435.
[7] G.D. O'Neil, S. Ahmed, K. Halloran, J.N. Janusz, A. Rodríguez, I.M. Terrero Rodríguez, Single-step fabrication of electrochemical flow cells utilizing multi-material 3D printing, Electrochem. Commun. 99 (2019) 56–60, https://doi.org/10.1016/j.elecom.2018.12.006.
[8] G. Gaal, M. Mendes, T.P. de Almeida, M.H.O. Piazzetta, Â.L. Gobbi, A. Riul, V. Rodrigues, Simplified fabrication of integrated microfluidic devices using fused deposition modeling 3D printing, Sens. Actuators, B 242 (2017) 35–40, https://doi.org/10.1016/j.snb.2016.10.110.
[9] R.M. Cardoso, D.M.H. Mendonça, W.P. Silva, M.N.T. Silva, E. Nossol, R.A.B. da Silva, E.M. Richter, R.A.A. Muñoz, 3D printing for electroanalysis: From multiuse electrochemical cells to sensors, Anal. Chim. Acta 1033 (2018) 49–57, https://doi.org/10.1016/j.aca.2018.06.021.
[10] R.M. Cardoso, P.R.L. Silva, A.P. Lima, D.P. Rocha, T.C. Oliveira, T.M. do Prado, E. L. Fava, O. Fatibello-Filho, E.M. Richter, R.A.A. Muñoz, 3D-printed graphene/polylactic acid electrode for bioanalysis: Biosensing of glucose and simultaneous determination of uric acid and nitrite in biological fluids, Sens. Actuators, B 307 (2020) 127621, https://doi.org/10.1016/j.snb.2019.127621.
[11] C.W. Foster, M.P. Down, Y. Zhang, X. Ji, S.J. Rowley-Neale, G.C. Smith, P.J. Kelly, C.E. Banks, 3D printed graphene based energy storage devices, Sci. Rep. 7 (2017) 42233, https://doi.org/10.1038/srep42233.
[12] R. Gómez-Hernández, Y. Panecatl-Bernal, M.Á. Méndez-Rojas, High yield and simple one-step production of carbon black nanoparticles from waste tires, Heliyon. 5 (7) (2019) e02139, https://doi.org/10.1016/j.heliyon.2019.e02139.
[13] A.F. João, A.L. Squissato, E.M. Richter, R.A.A. Muñoz, Additive-manufactured sensors for biofuel analysis: copper determination in bioethanol using a 3D-printed carbon black/polylactic electrode, Anal. Bioanal. Chem. 412 (12) (2020) 2755–2762, https://doi.org/10.1007/s00216-020-02513-y.
[14] V. Katseli, N. Thomaidis, A. Economou, C. Kokkinos, Miniature 3D-printed integrated electrochemical cell for trace voltammetric Hg(II) determination, Sens. Actuators, B 308 (2020) 127715, https://doi.org/10.1016/j.snb.2020.127715.
[15] V. Katseli, A. Economou, C. Kokkinos, Single-step fabrication of an integrated 3D-printed device for electrochemical sensing applications, Electrochem. Commun. 103 (2019) 100–103, https://doi.org/10.1016/j.elecom.2019.05.008.
[16] D.P. Rocha, A.L. Squissato, S.M. da Silva, E.M. Richter, R.A.A. Munoz, Improved electrochemical detection of metals in biological samples using 3D-printed electrode: Chemical/electrochemical treatment exposes carbon-black conductive sites, Electrochim. Acta 335 (2020) 135688, https://doi.org/10.1016/j.electacta.2020.135688.
[17] E.M. Richter, D.P. Rocha, R.M. Cardoso, E.M. Keefe, C.W. Foster, R.A.A. Munoz, C. E. Banks, Complete additively manufactured (3D-printed) electrochemical sensing platform, Anal. Chem. 91 (20) (2019) 12844–12851, https://doi.org/10.1021/acs.analchem.9b0257310.1021/acs.analchem.9b02573.s001.
[18] M.P. Browne, F. Novotný, Z. Sofer, M. Pumera, 3D printed graphene electrodes' electrochemical activation, ACS Appl. Mater. Interfaces 10 (46) (2018) 40294–40301, https://doi.org/10.1021/acsami.8b1470110.1021/acsami.8b14701.s001.
[19] S.H. Lee, W.S. Song, Enzymatic hydrolysis of polylactic acid fiber, Appl. Biochem. Biotechnol. 164 (1) (2011) 89–102, https://doi.org/10.1007/s12010-010-9117-7.
[20] C.L. Manzanares-Palenzuela, S. Hermanova, Z. Sofer, M. Pumera, Proteinase-sculptured 3D-printed graphene/polylactic acid electrodes as potential biosensing platforms: towards enzymatic modeling of 3D-printed structures, Nanoscale. 11 (25) (2019) 12124–12131, https://doi.org/10.1039/C9NR02754H.
[21] M.J. Glowacki, M. Cieslik, M. Sawczak, A. Koterwa, I. Kaczmarzyk, R. Jendrzejewski, L. Szynkiewicz, T. Ossowski, R. Bogdanowicz, P. Niedzialkowski, J. Ryl, Helium-assisted, solvent-free electro-activation of 3D printed conductive carbon-polylactide electrodes by pulsed laser ablation, Appl. Surf. Sci. 556 (2021) 149788, https://doi.org/10.1016/j.apsusc.2021.149788.
[22] D.P. Rocha, R.G. Rocha, S.V.F. Castro, M.A.G. Trindade, R.A.A. Munoz, E. M. Richter, L. Angnes, Posttreatment of 3D-printed surfaces for electrochemical applications: A critical review on proposed protocols, Electrochem. Sci. Adv. (2021), https://doi.org/10.1002/elsa.202100136.
[23] P. Chen, R.L. McCreery, Control of electron transfer kinetics at glassy carbon electrodes by specific surface modification, Anal. Chem. 68 (22) (1996) 3958–3965, https://doi.org/10.1021/ac960492r.
[24] M. Janik, P. Niedziałkowski, K. Lechowicz, M. Koba, P. Sezemsky, V. Stranak, T. Ossowski, M. Śmietana, Electrochemically directed biofunctionalization of a lossy-mode resonance optical fiber sensor, Opt. Express 28 (11) (2020) 15934, https://doi.org/10.1364/OE.390780.
[25] R.S. Nicholson, Theory and application of cyclic voltammetry for measurement of electrode reaction kinetics, Anal. Chem. 37 (11) (1965) 1351–1355, https://doi.org/10.1021/ac60230a016.
[26] J. Ryl, L. Burczyk, A. Zielinski, M. Ficek, A. Franczak, R. Bogdanowicz, K. Darowicki, Heterogeneous oxidation of highly boron-doped diamond electrodes and its influence on the surface distribution of electrochemical activity, Electrochim. Acta 297 (2019) 1018–1027, https://doi.org/10.1016/j.electacta.2018.12.050.

[27] J. Heinze, Cyclovoltammetrie — die „Spektroskopie" des Elektrochemikers, Angew. Chem. 96 (11) (1984) 823–840, https://doi.org/10.1002/(ISSN)1521-375710.1002/ange.v96:1110.1002/ange.19840961104.
[28] C. Kalinke, N.V. Neumsteir, G.d.O. Aparecido, T.V.d.B. Ferraz, P.L. dos Santos, B. C. Janegitz, J.A. Bonacin, Comparison of activation processes for 3D printed PLA-graphene electrodes: electrochemical properties and application for sensing of dopamine, Analyst. 145 (4) (2020) 1207–1218, https://doi.org/10.1039/C9AN01926J.
[29] T.J. Davies, C.E. Banks, R.G. Compton, Voltammetry at spatially heterogeneous electrodes, J. Solid State Electrochem. 9 (12) (2005) 797–808, https://doi.org/10.1007/s10008-005-0699-x.
[30] P. Niedziałkowski, M. Bojko, J. Ryl, A. Wcisło, M. Spodzieja, K. Magiera-Mularz, K. Guzik, G. Dubin, T.A. Holak, T. Ossowski, S. Rodziewicz-Motowidło, Ultrasensitive electrochemical determination of the cancer biomarker protein sPD-L1 based on a BMS-8-modified gold electrode, Bioelectrochemistry 139 (2021) 107742, https://doi.org/10.1016/j.bioelechem.2021.107742.
[31] P. Niedzialkowski, P. Slepski, J. Wysocka, J. Chamier-Cieminska, L. Burczyk, M. Sobaszek, A. Wcislo, T. Ossowski, R. Bogdanowicz, J. Ryl, Multisine impedimetric probing of biocatalytic reactions for label-free detection of DEFB1 gene: How to verify that your dog is not human? Sens. Actuators, B 323 (2020) 128664, https://doi.org/10.1016/j.snb.2020.128664.
[32] B. Hirschorn, M.E. Orazem, B. Tribollet, V. Vivier, I. Frateur, M. Musiani, Determination of effective capacitance and film thickness from constant-phase-element parameters, Electrochim. Acta 55 (21) (2010) 6218–6227, https://doi.org/10.1016/j.electacta.2009.10.065.
[33] M. Sobaszek, K. Siuzdak, M. Sawczak, J. Ryl, R. Bogdanowicz, Fabrication and characterization of composite TiO2 nanotubes/boron-doped diamond electrodes towards enhanced supercapacitors, Thin Solid Films 601 (2016) 35–40, https://doi.org/10.1016/j.tsf.2015.09.073.
[34] D.P. Rocha, V.N. Ataide, A. de Siervo, J.M. Gonçalves, R.A.A. Muñoz, T.R.L. C. Paixão, L. Angnes, Reagentless and sub-minute laser-scribing treatment to produce enhanced disposable electrochemical sensors via additive manufacture, Chem. Eng. J. 425 (2021) 130594, https://doi.org/10.1016/j.cej.2021.130594.
[35] S. Evans, Correction for the effects of adventitious carbon overlayers in quantitative XPS analysis, Surface and Interface, Analysis. 25 (1997) 924–930, https://doi.org/10.1002/(SICI)1096-9918(199711)25:12<924::AID-SIA317>3.0.CO;2-2.
[36] D. Pantea, H. Darmstadt, S. Kaliaguine, C. Roy, Electrical conductivity of conductive carbon blacks: influence of surface chemistry and topology, Appl. Surf. Sci. 217 (1-4) (2003) 181–193, https://doi.org/10.1016/S0169-4332(03)00550-6.
[37] P. Niedziałkowski, T. Ossowski, P. Zięba, A. Cirocka, P. Rochowski, S. J. Pogorzelski, J. Ryl, M. Sobaszek, R. Bogdanowicz, Poly-l-lysine-modified boron-doped diamond electrodes for the amperometric detection of nucleic acid bases, J. Electroanal. Chem. 756 (2015) 84–93, https://doi.org/10.1016/j.jelechem.2015.08.006.
[38] K. Ghosh, S. Ng, C. Iffelsberger, M. Pumera, Inherent impurities in graphene/polylactic acid filament strongly influence on the capacitive performance of 3D-printed electrode, Chem. Eur. J. 26 (67) (2020) 15746–15753, https://doi.org/10.1002/chem.v26.6710.1002/chem.202004250.
[39] J. Ryl, J. Wysocka, M. Cieslik, H. Gerengi, T. Ossowski, S. Krakowiak, P. Niedzialkowski, Understanding the origin of high corrosion inhibition efficiency of bee products towards aluminium alloys in alkaline environments, Electrochim. Acta 304 (2019) 263–274, https://doi.org/10.1016/j.electacta.2019.03.012.
[40] J.F.S. Pereira, R.G. Rocha, S.V.F. Castro, A.F. João, P.H.S. Borges, D.P. Rocha, A. de Siervo, E.M. Richter, E. Nossol, R.V. Gelamo, R.A.A. Muñoz, Reactive oxygen plasma treatment of 3D-printed carbon electrodes towards high-performance electrochemical sensors, Sens. Actuators, B 347 (2021) 130651, https://doi.org/10.1016/j.snb.2021.130651.
[41] E. Vaněčková, M. Bouša, Š. Nováková Lachmanová, J. Rathouský, M. Gál, T. Sebechlebská, V. Kolivoška, 3D printed polylactic acid/carbon black electrodes with nearly ideal electrochemical behaviour, J. Electroanal. Chem. 857 (2020) 113745, https://doi.org/10.1016/j.jelechem.2019.113745.
[42] Y. Yamada, J. Kim, S. Matsuo, S. Sato, Nitrogen-containing graphene analyzed by X-ray photoelectron spectroscopy, Carbon 70 (2014) 59–74, https://doi.org/10.1016/j.carbon.2013.12.061.
[43] J.H. Jung, M. Ree, H. Kim, Acid- and base-catalyzed hydrolyses of aliphatic polycarbonates and polyesters, Catal. Today 115 (1-4) (2006) 283–287, https://doi.org/10.1016/j.cattod.2006.02.060.
[44] N. Lucas, C. Bienaime, C. Belloy, M. Queneudec, F. Silvestre, J.-E. Nava-Saucedo, Polymer biodegradation: Mechanisms and estimation techniques – A review, Chemosphere 73 (4) (2008) 429–442, https://doi.org/10.1016/j.chemosphere.2008.06.064.
[45] S.J. de Jong, E.R. Arias, D.T.S. Rijkers, C.F. van Nostrum, J.J. Kettenes-van den Bosch, W.E. Hennink, New insights into the hydrolytic degradation of poly(lactic acid): participation of the alcohol terminus, Polymer 42 (7) (2001) 2795–2802, https://doi.org/10.1016/S0032-3861(00)00646-7.
[46] Q. Huang, M. Hiyama, T. Kabe, S. Kimura, T. Iwata, Enzymatic self-biodegradation of poly(L-lactic acid) films by embedded heat-treated and immobilized proteinase K, Biomacromolecules 21 (2020) 3301–3307, https://doi.org/10.1021/acs.biomac.0c00759.
[47] H. Tsuji, S. Miyauchi, Enzymatic hydrolysis of poly(lactide)s: effects of molecular weight, L-lactide content, and enantiomeric and diastereoisomeric polymer blending, Biomacromolecules 2 (2001) 597–604, https://doi.org/10.1021/bm010048k.
[48] W. Saenger, K. Proteinase, Handbook of Proteolytic Enzymes, Elsevier (2013) 3240–3242, https://doi.org/10.1016/B978-0-12-382219-2.00714-6.
[49] C. Lorena Manzanares Palenzuela, Filip Novotný, Petr Krupička, Zdeněk Sofer, Martin Pumera, 3D-printed graphene/polylactic acid electrodes promise high sensitivity in electroanalysis, Anal. Chem. 90 (9) (2018) 5753–5757, https://doi.org/10.1021/acs.analchem.8b0008310.1021/acs.analchem.8b00083.s001.
[50] Hideto Tsuji, Yoshio Kawashima, Hirofumi Takikawa, Saburo Tanaka, Poly(l-lactide)/nano-structured carbon composites: Conductivity, thermal properties, crystallization, and biodegradation, Polymer 48 (14) (2007) 4213–4225, https://doi.org/10.1016/j.polymer.2007.05.040.
[51] Scott D. Kimmins, Paul Wyman, Neil R. Cameron, Amine-functionalization of glycidyl methacrylate-containing emulsion-templated porous polymers and immobilization of proteinase K for biocatalysis, Polymer 55 (1) (2014) 416–425, https://doi.org/10.1016/j.polymer.2013.09.019.
[52] P. Niedziałkowski, R. Bogdanowicz, P. Zięba, J. Wysocka, J. Ryl, M. Sobaszek, T. Ossowski, Melamine-modified boron-doped diamond towards enhanced detection of adenine, guanine and caffeine, Electroanalysis 28 (1) (2016) 211–221, https://doi.org/10.1002/elan.v28.110.1002/elan.201500528.
[53] Y. Oda, A. Yonetsu, T. Urakami, K. Tonomura, Degradation of polylactide by commercial proteases, J. Polym. Environ. 8 (2000) 29–32, https://doi.org/10.1023/A:1010120128048.
[54] X. Qi, Y. Ren, X. Wang, New advances in the biodegradation of Poly(lactic) acid, Int. Biodeterior. Biodegrad. 117 (2017) 215–223, https://doi.org/10.1016/j.ibiod.2017.01.010.
[55] Fusako Kawai, Kosuke Nakadai, Emiko Nishioka, Hajime Nakajima, Hitomi Ohara, Kazuo Masaki, Haruyuki Iefuji, Different enantioselectivity of two types of poly (lactic acid) depolymerases toward poly(l-lactic acid) and poly(d-lactic acid), Polym. Degrad. Stab. 96 (7) (2011) 1342–1348, https://doi.org/10.1016/j.polymdegradstab.2011.03.022.
[56] S.B. Larson, J.S. Day, C. Nguyen, R. Cudney, A. McPherson, High-resolution structure of proteinase K cocrystallized with digalacturonic acid, Acta Crystallogr. F Struct. Biol. Cryst. Commun. 65 (2009) 192–198, https://doi.org/10.1107/S1744309109002218.
[57] Christian Betzel, S. Gourinath, Pravindra Kumar, Punit Kaur, Markus Perbandt, Susanne Eschenburg, Tej P. Singh, Structure of a serine protease proteinase K from *Tritirachium album limber* at 0.98 Å resolution, Biochemistry 40 (10) (2001) 3080–3088, https://doi.org/10.1021/bi002538n.
[58] Wei Zhao, Ruijin Yang, Experimental study on conformational changes of lysozyme in solution induced by pulsed electric field and thermal stresses, J. Phys. Chem. B 114 (1) (2010) 503–510, https://doi.org/10.1021/jp9081189.
[59] Yueming Tan, Wenfang Deng, Chao Chen, Qingji Xie, Lihong Lei, Yunyong Li, Zhengfa Fang, Ming Ma, Jinhua Chen, Shouzhuo Yao, Immobilization of enzymes at high load/activity by aqueous electrodeposition of enzyme-tethered chitosan for highly sensitive amperometric biosensing, Biosens. Bioelectron. 25 (12) (2010) 2644–2650, https://doi.org/10.1016/j.bios.2010.04.040.
[60] Jesús E. Contreras-Naranjo, Victor H. Perez-Gonzalez, Marco A. Mata-Gómez, Oscar Aguilar, 3D-printed hybrid-carbon-based electrodes for electroanalytical sensing applications, Electrochem. Commun. 130 (2021) 107098, https://doi.org/10.1016/j.elecom.2021.107098.
[61] G. Martins, J.L. Gogola, L.H. Budni, B.C. Janegitz, L.H. Marcolino-Junior, M. F. Bergamini, 3D-printed electrode as a new platform for electrochemical immunosensors for virus detection, Anal. Chim. Acta 1147 (2021) 30–37, https://doi.org/10.1016/j.aca.2020.12.014.
[62] Filip Novotný, Veronika Urbanová, Jan Plutnar, Martin Pumera, Preserving fine structure details and dramatically enhancing electron transfer rates in graphene 3D-printed electrodes via thermal annealing: toward nitroaromatic explosives sensing, ACS Appl. Mater. Interfaces 11 (38) (2019) 35371–35375, https://doi.org/10.1021/acsami.9b0668310.1021/acsami.9b06683.s001.